New theophylline-activated Diels–Alderase ribozymes by molecular engineering

Markus Petermeier and Andres Jäschke*

Received 24th September 2008, Accepted 21st October 2008
First published as an Advance Article on the web 20th November 2008
DOI: 10.1039/b816726e

Allosteric ribozymes were developed by rational design and step-wise optimization. These ribozymes accelerate a Diels–Alder reaction between anthracene and maleimide derivatives. The optimized sequence is efficiently activated by theophylline under single and multiple turnover conditions and distinguishes between structurally similar effector molecules.

Introduction

The reversible control of chemical reaction rates by external trigger signals is of great interest both from a fundamental and an application perspective. Catalytic reactions are particularly attractive, and Nature has evolved elaborate mechanisms of allostery to control enzymatic reaction rates by the concentration of effector molecules.[1] Catalytic ribonucleic acids (ribozymes) have been successfully converted into allosteric systems by combinatorial selection or by rational design,[2–6] but to our knowledge, there are only two reports on allosterically controlled ribozymes for "small-molecule chemistry" (*i.e.*, reactions different from RNA cleavage or ligation).[7,8]

Our lab has previously discovered a ribozyme that catalyzes the formation of C–C bonds by Diels–Alder reaction (Fig. 1a) and characterized this ribozyme extensively.[9–14] The high amount of structural information available (including X-ray crystal structures) arguably make the Diels–Alderase ribozyme the best-characterized artificial ribozyme known to-date, and render it attractive for the development of allosteric systems. We previously reported the development of allosterically controlled Diels–Alderase ribozymes by combinatorial selection,[8] and by rational design,[7] utilizing well-described RNA aptamer sequences as recognition modules.

In the rational design study, we introduced the concept of direct inactivating interference.[7] The operating principle is the stabilization of catalytically inactive conformations by direct interference of sequence elements of both domains (*i.e.*, aptamer and ribozyme). On binding the effector (*i.e.*, the molecule to be recognized by the aptamer), this stabilizing interference is overcome and the RNA refolds into a catalytically active conformation (Fig. 1). This approach uses complementary stretches of nucleotides that are either already present in the parental aptamer and ribozyme sequences or can be incorporated at weakly conserved positions by mutation. Through multiple rounds of design and testing, the relative stabilities of the competing active and inactive structures can be optimized and fine-tuned, and allosteric systems for two pharmaceutically relevant analytes (theophylline and tobramycine) were developed that exhibited

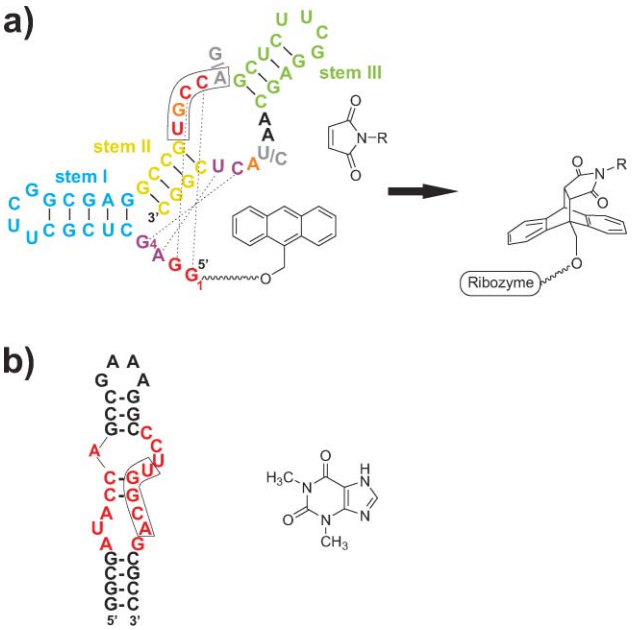

Fig. 1 RNA molecules utilized in the design of allosteric ribozymes. A) Secondary structure of the Diels–Alderase ribozyme and catalyzed reaction. Green and blue stem-loop structures are completely variable in size and sequence, while the yellow helix is variable in sequence, but conserved in size. Nucleotides in red are invariant, orange: highly conserved (over 90% activity reduction on mutation). Purple: pair-wise complementary substitutions allowed. Gray: strong preference for two nucleotides. Black: variable (less than 50% activity reduction on mutation). Black dotted lines: Watson–Crick pseudoknot base pairs. B) Theophylline aptamer secondary structure (conserved residues in red, variable in black), and effector formula.

~50-fold activation by the effector ligand under single-turnover conditions.[7] Their performance under true catalytic conditions (*i.e.*, multiple turnover) is, however, not known.

In this previous study the two different aptamer modules were attached to the upper part of the ribozyme, thereby replacing stem III (see Fig. 1a). To test whether the approach of direct inactivating interference is generally applicable or whether it is limited to carefully selected cases, we now modify a different part of the ribozyme molecule. Using the Diels–Alderase ribozyme as the catalytic platform, we now replace helix I by the theophylline aptamer[15] (Fig. 1b) and use weakly conserved sequence elements

Institute of Pharmacy and Molecular Biotechnology, University of Heidelberg, Im Neuenheimer Feld 364, D-69120, Heidelberg, Germany. E-mail: jaeschke@uni-hd.de; Fax: +49 6221 546430; Tel: +49 6221 544851

in both domains to design alternative structures. The ability to attach regulatory modules to different positions of a catalyst is an important precondition for the development of logic gates[16] in which multiple sensor modules are attached to the Diels–Alderase ribozyme.

Results and discussion

1. Initial design

For both the Diels–Alderase ribozyme and the theophylline aptamer, extensive mutational data are available that define conserved and variable positions (see color coding in Fig. 1).[9,15] Most important for rational design, the two RNA molecules contain a complementary five-nucleotide stretch (UGCCA in the ribozyme, UGGCA in the aptamer, boxes in Fig. 1), which could be utilized to induce an inter-domain interaction. For the design of the allosteric system, stem I of the ribozyme is replaced by a truncated version of the aptamer, keeping the ribozyme's 5′-GGAG end that is important for pseudoknot formation of the Diels–Alderase (dotted lines in Fig. 1a). Stem III, adjacent to the ribozyme's UGCCA stretch, is only weakly conserved, allowing extension of the inter-domain inactivator to 7 base-pairs by mutation (yellow boxes in Fig. 2, construct Theo 1). The

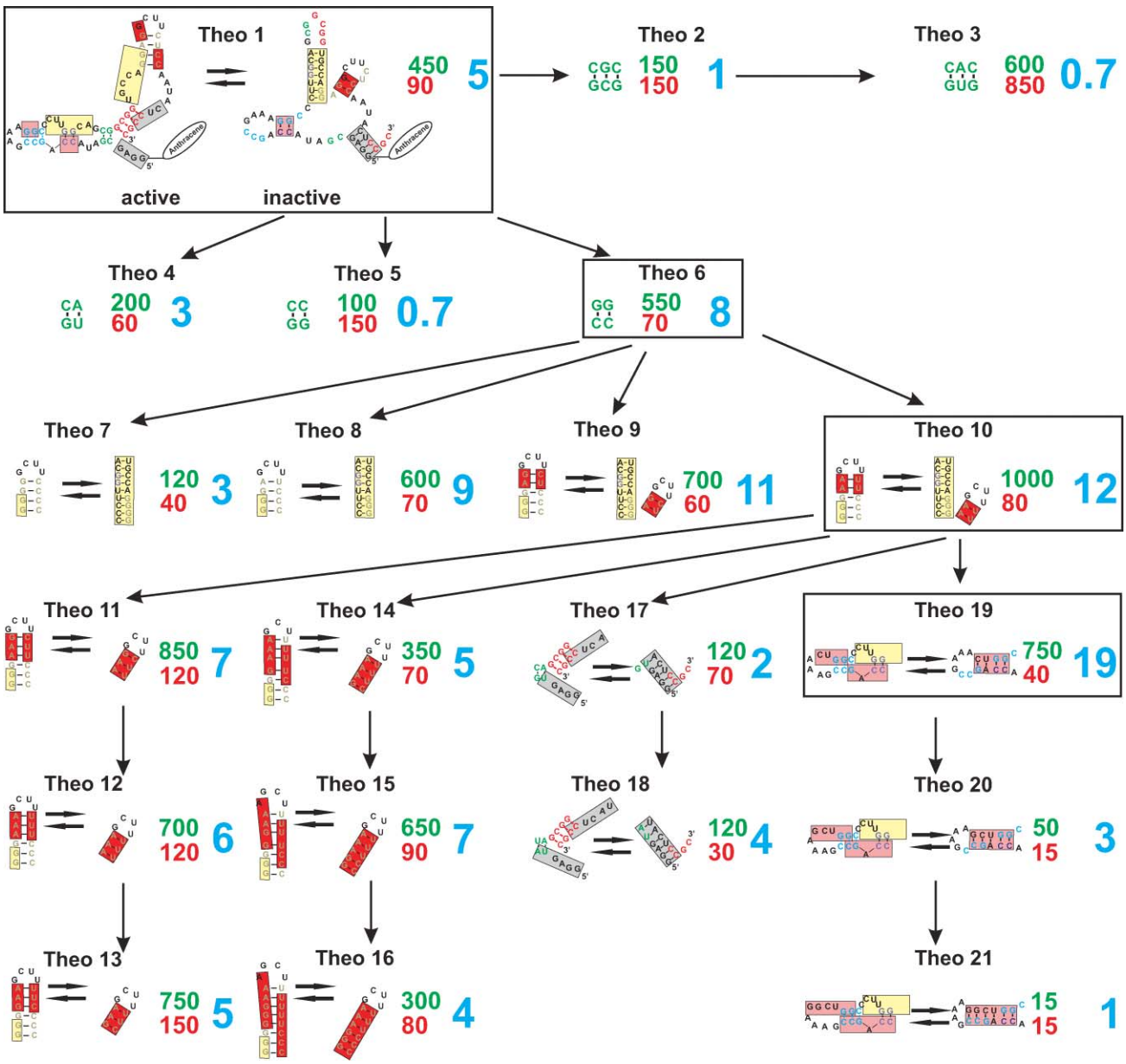

Fig. 2 Design of theophylline-dependent Diels–Alderase ribozymes. The Diels–Alderase ribozyme and the theophylline aptamer are fused after removing helix I (ribozyme) and the lower aptamer helix (see Fig. 1). Colored boxes indicate interactions that are assumed to stabilize the inactive structure, while colored letters show interactions that should stabilize the active structure. Only those parts of the structure are shown that change compared to the ancestor. Green numbers indicate initial rate in the presence of 1 mM theophylline (nM/min), red in the absence, and blue the allosteric switching factor, defined as the ratio of the two rates.

ribozyme's 3′-end (helix II) is mutated so that it can alternatively pair with the 5′-terminal GGAG (grey box), and a second potential inactivator element was incorporated by design (orange box). The aptamer also contains a sequence element that could lead to an alternative fold (pink box). As in a previous study connection of the aptamer and ribozyme modules by a 2 bp helix was found to work best, the initial design included such a connector (green letters). Thus, the initial construct Theo 1 is 64 nt long and designed to switch between two different structures. In the absence of theophylline, the inactive structure should be favored, which is stabilized by four different double-strand interactions (colored boxes), while binding of theophylline should induce folding into the active structure, which is stabilized by five stems (colored letters).

Theo 1 as well as all other constructs was enzymatically synthesized, using transcription initiation to attach a deca(ethylene glycol)-tethered anthracene to the RNA's 5′-end.[10] The rate of the ribozyme-catalyzed Diels–Alder reaction was determined in a fluorescence-based screening assay in the absence or presence (1 mM) of theophylline by measuring the time required to achieve conversion of 10% of the tethered anthracene.

2. Optimization

Starting construct Theo 1 showed high catalytic activity and already significant allostericity, as the reaction rate was about 5 times higher in the presence of theophylline than in the absence (Fig. 2). This not only supports our design assumptions but also confirms the feasibility of the rational design approach itself.

Optimization proceeded in four steps: connector tuning (constructs Theo 2–6), optimization of the inter-domain inactivator (Theo 7–10), variation of intra-ribozyme interactions (Theo 11–18), and tuning of intra-aptamer interactions (Theo 19–21). Increasing the length of the connector stem from 2 to 3 bp reduced allostericity (Theo 2,3). Among the four different 2 bp connectors tested, the GG:CC combination worked best (Theo 6, switching factor 8).

Variations of the inter-domain inactivator (yellow box, 7 bp) often influence helix III (olive letters, 4 bp) at the same time. If the inactivator is too stable (9 bp, Theo 7), catalytic activity and allostericity are significantly reduced. A length of 8 bp seems to be ideal (Theo 8, switching factor 9), while addition of a fifth base-pair to helix III further improves performance (Theo 9 and 10, switching factors 11 and 12). We next turned to tune the intra-ribozyme interactions. Addition of a 6th base pair to helix III, thought to stabilize the catalytically active form, was found to slightly reduces the rate in the presence of effector, and to more severely increase the rate in its absence (Theo 11–13). The elongation of the orange box intra-ribozyme inactivator stabilized the inactive structure, but did this likewise in the absence and presence of effector (Theo 14–16). Increasing the stability of the grey intra-ribozyme inactivator box lead to inactivation and reduction of allostericity (Theo 17, 18), apparently causing a too strong stabilization of the inactive form. Thus, tuning of intra-ribozyme interactions did not lead to any improvement of allostericity. Elongation of the pink intra-aptamer inactivator, however, from 2 to 4 bp selectively reduced the activity in the absence of theophylline (by a factor of 3) with little effect on the rate in its presence, yielding construct Theo 19, which showed the highest measured switching factor of 19. Further elongation, however, leads to inactivation (Theo 20 and 21).

Thus, the step-wise optimization process improved allostericity about 3.5-fold, compared to the rationally designed initial construct. The rate in the absence of effector was reduced, while it was increased in its presence. Apparently, RNA Theo 19 provides the optimal balance of stabilities of the active and inactive conformations to allow effector binding to shift the equilibrium from the inactive towards the catalytically active conformation. This molecule was characterized in more detail both under single- and multiple turnover conditions.

3. Allostericity and selectivity

The dependence of the single-turnover rate of the Diels–Alder reaction of tethered anthracene was measured by fluorescence spectroscopy as a function of theophylline concentration. Anthracene is a sensitive fluorophore, and the Diels–Alder reaction leads to complete loss of fluorescence. Initial rates were determined by least-square regression from the fluorescence-time curves recorded for 365 nm excitation and 419 nm emission. The allosteric ribozyme was found to exhibit excellent allostericity. In the absence of effector, a rate of 10 nM/min is measured, and upon addition of theophylline, the reaction rate increases with the analyte concentration, showing typical saturation behavior (Fig. 3). The highest activity measured is ~540 nM/min, corresponding to a 54-fold allosteric activation of the catalyst by the effector. Anthracene fluorescence decays in an exponential manner (Fig. 3b). The half-maximal rate is reached at a theophylline concentration of ~70 μM. The structurally similar analyte caffeine which differs from theophylline only by one methyl group does not induce any rate acceleration up to the highest measured concentration of 1 mM, thereby demonstrating the high selectivity of this allosteric catalyst.

4. Multiple-turnover catalysis

To assess the performance of the system under true catalytic conditions (*i.e.*, using free anthracene and maleimide substrates under multiple turnover conditions), HPLC measurements were carried out that directly monitor the formation of Diels–Alder product between 100 μM anthracene–hexaethylene glycol and 500 μM *N*-pentylmaleimide in the absence or presence of 21 μM RNA Theo 19 in reaction buffer (Fig. 4). After 1 hour, the area of the Diels–Alder product peak indicates that 54% of the anthracene have been converted in the presence of RNA and theophylline, corresponding to 2.5 turnovers per catalyst molecule (Fig. 4, trace 4). For the precise determination of initial rates, aliquots were withdrawn within the first 5% of conversion, analyzed by HPLC, and the peak areas quantified. The rate of the uncatalyzed background reaction (no RNA, no theophylline) was found to be 70 nM/min, and addition of theophylline yielded the same value. In the absence of theophylline, RNA Theo 19 caused a slight acceleration (110 nM/min). Addition of 100 μM theophylline, however, caused a 6-fold overall acceleration (650 nM/min), and subtraction of the background rates yielded a background-corrected switching factor of 14, demonstrating efficient activation of the catalytic Diels–Alder reaction.

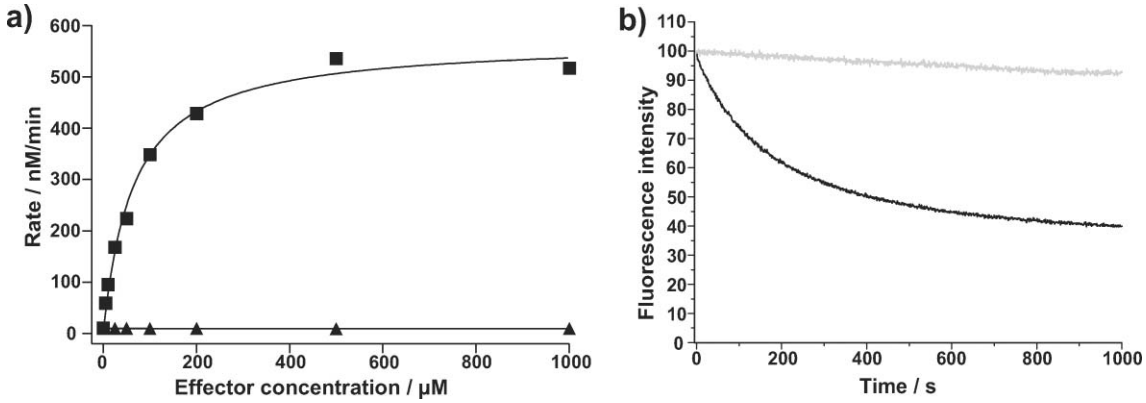

Fig. 3 Single-turnover Diels–Alder catalysis by RNA Theo 19: a) Dependence of the reaction rates on the concentration of theophylline (squares) and caffeine (triangles) in the absence and presence of 1 mM effector (unless otherwise stated). b) Fluorescence–time curves for the reaction at 0 (gray) and 1 mM (black) theophylline.

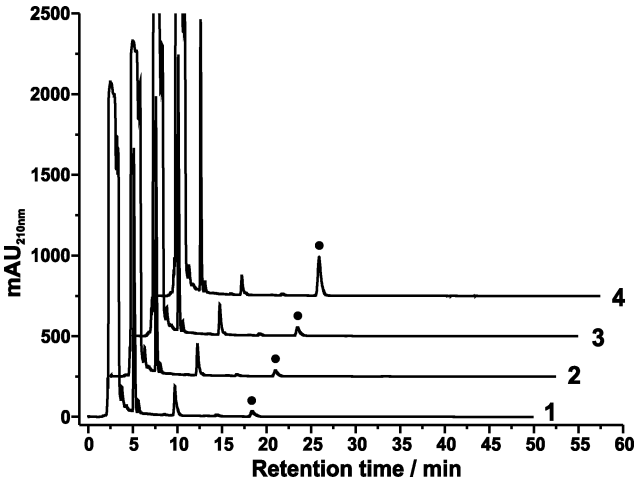

Fig. 4 HPLC analysis of multiple turnover reactions after 1 hour reaction time (trace 1: background, 2: background plus 100 μM theophylline, 3: reaction catalyzed by 21 μM RNA Theo 19, 4: reaction catalyzed by 21 μM RNA Theo 19 plus 100 μM theophylline). The dot indicates the Diels–Alder reaction product.

Conclusions

The allosteric ribozymes developed here by iterations of rational design and testing show strong allosteric activation by the effector in different assays, both in a single-turnover format and under true catalytic conditions. The ribozymes show excellent discrimination between structurally closely related analytes. In contrast to typical ribozyme-catalyzed RNA cleavage reactions, the consumption of anthracene in a Diels–Alder reaction generates UV and fluorescence signals without the requirement for labelling, rendering this system attractive for the development of assays for a variety of analytes.

This work demonstrates that the Diels–Alderase ribozyme, although known to have a remarkably stable tertiary architecture including a pre-formed catalytic pocket, can be coupled to effector recognition domains at different positions, and effector binding directly influences the catalytic performance of the ribozyme. The results obtained confirm the feasibility of the direct inactivating interference approach that uses simple design considerations for the rational construction of allosteric ribozymes.

Experimental

DNA Template preparation

DNA strands and primers were purchased from IBA, Göttingen or SIGMA-ALDRICH, Taufkirchen. Double-stranded (ds) DNA templates for T7 transcription were generated from synthetic single-stranded DNA templates (Theo 1–21) encoding the antisense sequence of the desired RNA sequence preceded by the T7 promoter. dsDNA was obtained through a fill up reaction using only the appropriate 3′-primer in stochiometric amounts in 67 mM Tris-HCl pH 8.8, 16 mM $(NH_4)_2SO_4$, 0.01% Tween 20 and 4 mM $MgCl_2$, 0.5 mM dNTP and 0.1 U/μl Taq polymerase (GenTherm™ DNA polymerase, Rapidozym, Berlin, Germany). The fill-up reaction was performed submitting both DNA oligomers at 10 μM final concentrations to incubation under the following PCR conditions: 20 cycles of 1 min at 90 °C, 1 min at 56 °C, and 1 min at 72 °C, followed by 10 min incubation at 72 °C and subsequent cooling to 0 °C.

Enzymatic RNA synthesis

T7 in vitro transcriptions were performed in 80 mM Tris-HEPES pH 7.5, 22 mM $MgCl_2$, 1 mM spermidine, 10 mM DTT, 0.04 mg/ml BSA with 4 mM of each nucleoside triphosphate, 0.4 μCi/μl of radiolabeled α-^{32}P-CTP, 10 U/μl of T7 RNA polymerase (Fermentas, St. Leon-Rot), containing 20% (v/v) of the fill-up reaction mixture. For the synthesis of anthracene–decaethylene glycol–RNA conjugates, 4 mM of initiator nucleotide, anthracene–decaethylene glycol guanosine, were added and the guanosine triphosphate concentration was reduced to 1 mM. The incorporation of initiator nucleotide was monitored by HPLC analysis of an aliquot on an RP-18 column for each transcription reaction and found to vary between 80–90%. After 3–4 h incubation at 37 °C, the reaction mixture was mixed with one volume of loading buffer, purified by denaturing PAGE and visualized by autoradiography. Product bands were excised and eluted by agitation in 0.5 M ammonium acetate pH 7

(r.t., overnight). The obtained RNA was dissolved in H_2O after ethanol precipitation.

Diels–Alder reactions

Generally, Diels–Alder reactions were performed in DA-buffer (30 mM Tris-HCl pH 7.4, 300 mM NaCl and 20 mM $MgCl_2$) and initiated by the addition of the maleimide as the last component.

Fluorescence measurements

Single turnover experiments (anthracene covalently attached to the ribozyme sequence) were conducted using 2.5 μM RNA containing ≥80% anthracene-carrying RNA as determined by HPLC analysis. Typical reaction conditions included 25 μM biotin maleimide (added from a 2 mM stock solution in DMSO) in the absence or in the presence of 1 mM theophylline at 25° C and in a final volume of 15 μL. Experiments aimed at establishing the dependence of the reaction rate on the effector concentration (theophylline or caffeine) were performed varying the effector concentration between 5 and 1000 μM. Fluorescence kinetics were determined on a Jasco FP-6500-fluorescence spectrophotometer. Anthracene fluorescence was excited at 365 nm and monitored at 419 nm. Fluorescence values were normalized to a starting value of 100. The time required for a 10% reduction of the initial fluorescence was converted into a reaction rate (nM/min). The values obtained in the absence and presence of theophylline were divided by each other giving the switch factor or activation factor for each construct.

HPLC measurements

Multiple turnover experiments (anthracene and maleimide substrates free in solution) were conducted using 21 μM allosteric ribozyme, 100 μM anthracene hexaethylene-glycol, and 500 μM *N*-pentylmaleimide (added from a 5 mM stock solution in ethanol) in a final volume of 70 μL. Reactions were quenched by addition of β-mercaptoethanol and analysed by HPLC (column Phenomenex® Luna 5U C18 4.6 × 250 mm, isocratic elution with acetonitrile/water 52:48). Peak identification and quantification was done using calibration curves. First, all reactions were allowed to proceed for 1 hour (Fig. 4), and based on the amount of product formed, reaction times were then adjusted to stay within 5% conversion in order to determine initial rates.

Acknowledgements

We gratefully acknowledge support by the Deutsche Forschungsgemeinschaft, HFSP, and the Fonds der Chemischen Industrie.

References

1 J. F. Swain and L. M. Gierasch, *Curr. Opin. Struct. Biol.*, 2006, **16**, 102.
2 J. S. Hartig, I. Grüne, S. H. Najafi-Shoushtari and M. Famulok, *J. Am. Chem. Soc.*, 2004, **126**, 722.
3 M. Iyo, H. Kawasaki and K. Taira, *Methods Mol. Biol.*, 2004, **252**, 257.
4 M. Koizumi, G. A. Soukup, J. N. Kerr and R. R. Breaker, *Nat. Struct. Biol.*, 1999, **6**, 1062.
5 S. K. Silverman, *RNA*, 2003, **9**, 377.
6 J. Tang and R. R. Breaker, *Chem. Biol.*, 1997, **4**, 453.
7 S. Amontov and A. Jäschke, *Nucleic Acids Res.*, 2006, **34**, 5032.
8 M. Helm, M. Petermeier, B. Ge, R. Fiammengo and A. Jäschke, *J. Am. Chem. Soc.*, 2005, **127**, 10492.
9 S. Keiper, D. Bebenroth, B. Seelig, E. Westhof and A. Jäschke, *Chem. Biol.*, 2004, **11**, 1217.
10 B. Seelig and A. Jäschke, *Chem. Biol.*, 1999, **6**, 167.
11 B. Seelig, S. Keiper, F. Stuhlmann and A. Jäschke, *Angew. Chem. Int. Ed. Engl.*, 2000, **39**, 4576.
12 A. Serganov, S. Keiper, L. Malinina, V. Tereshko, E. Skripkin, C. Höbartner, A. Polonskaia, A. T. Phan, R. Wombacher, R. Micura, Z. Dauter, A. Jäschke and D. J. Patel, *Nat. Struct. Mol. Biol.*, 2005, **12**, 218.
13 F. Stuhlmann and A. Jäschke, *J. Am. Chem. Soc.*, 2002, **124**, 3238.
14 R. Wombacher, S. Keiper, S. Suhm, A. Serganov, D. J. Patel and A. Jäschke, *Angew. Chem. Int. Ed. Engl.*, 2006, **45**, 2469.
15 R. D. Jenison, S. C. Gill, A. Pardi and B. Polisky, *Science*, 1994, **263**, 1425.
16 D. M. Kolpashchikov and M. N. Stojanovic, *J. Am. Chem. Soc.*, 2005, **127**, 11348.

